Catalysis Today 418 (2023) 114133

Contents lists available at ScienceDirect

Catalysis Today

journal homepage: www.elsevier.com/locate/cattod

One-pot lower olefins production from CO_2 hydrogenation

C. Coffano [a], A. Porta [a], C.G. Visconti [a,*], F. Rabino [b], G. Franzoni [b], B. Picutti [b], L. Lietti [a,*]

[a] Dipartimento di Energia, Politecnico di Milano, Via La Masa 34, 20156 Milano, Italy
[b] Tecnimont SpA (Maire Tecnimont Group), Via Gaetano De Castillia 6/A, 20124 Milano, Italy

ARTICLE INFO

Keywords:
CO_2 hydrogenation
Lower olefins
Methanol
Methanol-to-olefins
One-pot synthesis

ABSTRACT

In this work the one-pot conversion of CO_2 into lower olefins is investigated over a physical mixture of a methanol synthesis catalyst and a methanol-to-olefins (MTO) zeolite. First, the feasibility of the single reactions is tested at CO_2 to olefins conditions, i.e., high temperature and high H_2/CO_2 pressure, providing insights on the reaction mechanism and catalyst stability. The effects of the operating conditions are then analyzed over the individual samples, starting from CO_2/H_2 mixtures in the case of the methanol synthesis catalyst and from methanol in CO_2/H_2 in the case of the zeolite. The In_2O_3-ZrO_2 catalyst exhibits very good selectivity to methanol and high activity, reaching thermodynamic equilibrium above 380 °C. The zeolite sample showed high activity as well and the presence of high H_2 partial pressure consistently increases the zeolite lifetime at high temperatures, but also the paraffin selectivity at the expense of the olefins, especially at low space velocity. It is therefore clear that a trade-off should be identified when testing the bi-functional catalytic samples in order to guarantee high methanol formation and good olefins production in the one-pot process. Finally, a comparison between methanol-mediated and modified Fischer-Tropsch (MFT) routes is presented, highlighting strengths and weaknesses of each reaction pathway. In particular, CO must be reduced in the methanol-mediated route, while methane and C_{5+} hydrocarbons formation is the main issue for the MFT reaction.

1. Introduction

In order to reduce the effects of anthropogenic greenhouse gases in the atmosphere, CO_2 can be reutilized as an abundant and renewable carbon feedstock. However, due to its thermodynamical stability, its conversion requires high external energy inputs or highly reactive co-reactants [1]. In this respect, catalytic hydrogenation of CO_2 has been shown to be a versatile route to synthetize fuels and chemicals, among which lower olefins ($C_2^=$-$C_4^=$) are one of the most appealing product, given their high added-value and the possibility to use them as building blocks for polyolefins production, enabling the long-term fixation of CO_2 [2].

Different routes have been proposed for the direct CO_2 hydrogenation to hydrocarbons. A possibility is represented by the modified Fischer−Tropsch synthesis (MFT), which consists of two main consecutive reactions: reverse water gas shift (RWGS) reaction to produce CO from CO_2 followed by the further conversion of CO to hydrocarbons via Fischer−Tropsch reaction [3–5]. K-promoted Fe-based catalysts demonstrate interesting activity and selectivity, enabling the one-pot synthesis of lower olefins [3,6,7]. Per-pass CO_2 conversions around 40% can be attained, but the produced hydrocarbons inevitably follow the Anderson−Schulz−Flory (ASF) distribution resulting in the undesired formation of methane and heavier hydrocarbons (C_5^+), besides C_2 to C_4 hydrocarbons (paraffins and olefins) [3,8].

A possible alternative to the MFT is the so-called MeOH-mediated route, involving methanol as intermediate. In this case CO_2 is initially converted to methanol (CO_2 to methanol, CTM); methanol is then transformed into lower olefins according to the Methanol-to-Olefins (MTO) process. This reaction pathway does not follow the FT mechanism and the product formation does not obey the ASF distribution, allowing in principle to reduce the amount of methane and C_5^+ hydrocarbons and maximizing the formation of C_2-C_4 olefins. The reaction may occurs in two separate reactors; however, to make this route more appealing, reducing in principle both CAPEX and OPEX [9], the two steps can be carried out in a single reactor. This one-pot process requires materials with different functionalities to catalyse both the methanol synthesis and the MTO reaction. To date, these bifunctional catalytic materials involve a combination (physical mixture) of a methanol synthesis catalyst (based on Cu, Zn or In) with a methanol-to-olefins acidic zeolite (typically H-SAPO-34 or H-ZSM-5) [9–12]. Nevertheless,

* Corresponding authors.
E-mail addresses: carlo.visconti@polimi.it (C.G. Visconti), luca.lietti@polimi.it (L. Lietti).

https://doi.org/10.1016/j.cattod.2023.114133
Received 17 December 2022; Received in revised form 24 February 2023; Accepted 24 March 2023
Available online 25 March 2023
0920-5861/© 2023 The Authors. Published by Elsevier B.V. This is an open access article under the CC BY license (http://creativecommons.org/licenses/by/4.0/).

coupling the two processes is challenging, as they are looking in opposite directions in terms of operating conditions: methanol synthesis (CTM) is carried out at high pressure (i.e., ~80 bar) and at temperatures lower than 300 °C due to thermodynamic reasons, whereas the MTO reaction is conducted at low pressure (typically lower than 5 bar) and requires temperatures higher than 350 °C to promote C-C coupling. Therefore, a compromise in the operating conditions is needed to carry out the one-pot process. However, it has to be noted that a synergism can be exploited in principle by coupling the methanol synthesis and the MTO catalysts, since the MTO catalyst removes methanol formed in the first step, thus pushing the CO_2 conversion to methanol according to the Le Chatelier principle.

Active and selective catalytic materials are sought for the one-pot olefins synthesis form CO_2 according to the methanol-mediated route. Concerning the CH_3OH synthesis catalysts, copper-based materials are well-known active catalysts in traditional process from syngas and they have also been investigated as active materials in the methanol synthesis from CO_2 [13,14]. These catalysts are active and stable at temperatures below 300 °C; however, when used in combination with a MTO catalyst, they should be operated at much higher temperatures, in the range 350–400 °C, being such temperatures required for the synthesis of olefins from methanol over the zeolitic material. In fact, when copper-based catalysts are used in tandem with a zeolite for the one-pot CO_2-to-olefins (CTO) process, satisfactory olefins yields are initially obtained, which however rapidly decrease due to the sintering of the copper catalyst at the relatively high operating temperatures required for the olefins production and in the presence of relatively high water partial pressures [15]. Besides, Cu accelerates RWGS reaction via surface redox mechanism resulting in a large CO formation [15]. Other methanol synthesis catalysts have been proposed, e.g., zinc and zirconium mixed oxides [16–18], or In-based catalysts [12,19–22], these latter showing the most promising results. Indeed, in recent years Indium has become a buzzword in the methanol scientific community in view of its remarkable selectivity when using CO_2 as feedstock [23–26]. It has been suggested that the high low temperature methanol yields are enabled by oxygen vacancies in the lattice of indium oxide due to its partial surface reduction. These favour the activation of CO_2 and H_2 at low temperature, while decreasing the CO formation via RWGS [24]. In the case of the CTO process their higher stability could also be exploited [12,26]. In fact, In-based materials are appealing not only for their enhanced activity, but also because of their improved stability when coprecipitated with zirconium oxide, which acts as structural promoter to prevent sintering [24].

Concerning MTO catalysts, zeolites, and in particular SAPO-34 and ZSM-5, are active and selective materials. The characteristics of these catalysts, in particular the cavity network and dimensions, the distribution of acidic sites and the crystal size, affect the product selectivity. The channel dimensions have a great impact on the product distribution, indeed the reaction intermediates are formed and trapped inside the channels and, depending on the dimensions, only certain products can escape the zeolite matrix. For this reason, it is possible to push the selectivity toward lower olefins by adopting a catalyst with a precise topology. SAPO-34 has the CHA topology with 8 membered ring: it possesses regular cavities connected by narrow windows and it is high selective to ethylene and propylene [27–29]. On the other hand, ZSM-5 is a 10 membered ring zeolite with a MFI topology and larger channel intersections. These characteristics make H-ZSM-5 more selective to higher olefins and aromatics [30,31]. Aromatics formation within the zeolite plays an important role in the olefin formation mechanism, but is also responsible for the carbon deposition process leading to the fast deactivation of the catalyst at MTO conditions [30,32]. In the case of the one-pot CO_2 to olefins reaction, the deactivation process is expected to proceed at a much slower rate, due to the high partial pressure of H_2 and H_2O that can effectively slow down the coking process [33].

Although a number of studies recently appeared in the open literature on the direct transformation of CO_2 into lower olefins through the methanol-mediated route, many aspects of the reaction are still unresolved. In particular, the drawbacks and benefits originating due to the interaction of the methanol synthesis catalyst with the zeolite are still unclear and need to be further addressed. Accordingly, in this paper we have addressed the one-pot olefins synthesis through the methanol mediated route using a bifunctional system obtained by physically mixing a home-made In-Zr oxide catalyst with a commercial SAPO-34 zeolite. After a preliminary characterization of the materials through reactivity at atmospheric pressure (TPD and TPR), the reactivity of the two systems (CTM and MTO) have been studied individually in order to better rationalize the behaviour of the catalyst mixture (CTO). Finally, a comparison of the performances of the MeOH-mediated route with those of the modified FT is presented, highlighting strengths and weaknesses of each reaction route.

2. Experimental

2.1. Catalyst preparation

The home-made In_2O_3-ZrO_2 was prepared by coprecipitation in a jacketed reactor. For this purpose, $In(NO_3)_3 \bullet 4,5H_2O$ (10.35 g) and $ZrO(NO_3)_2 \bullet 5H_2O$ (11.3 g) were dissolved in 250 mL of deionized water under stirring. Separately, the precipitating solution was prepared by mixing 125 mL of NH_4OH (30 wt% in H_2O) and 375 mL of ethanol. This solution is added with a rate of 2.5 mL/min to the salts-containing solution at room temperature under stirring. At the end of the precipitation, the obtained slurry is heated to 80 °C (heating rate: 3 °C/min) and left under stirring for 30 min. The precipitate is filtered and washed with deionized water, until a neutral pH is reached; eventually the solid is dried at 65 °C overnight. The thermogravimetric analysis in He flow of the dried co-precipitated precursor In-Zr sample is shown in Fig. S1a. During the test, the In-Zr sample shows a significant mass loss below 300 °C, associated with two endothermic phenomena at 150 and 250 °C, associated with the evolution in the gas phase of CO_2 and water that are associated with the transition of the precipitated hydroxy-carbonates to oxides. Prior to characterization and testing in the experimental rig, the sample was calcined in static air at 500 °C (heating rate: 2 °C/min) for 3 h.

Reference pure In_2O_3 and ZrO_2 have been obtained by using the same procedure, starting from pure In or Zr nitrate precursors. $In(NO_3)_3 \bullet 4,5H_2O$ (4.13 g) or $ZrO(NO_3)_2 \bullet 5H_2O$ (9.13 g) are dissolved in 50 mL of deionized water under stirring. The precipitating solution is composed by 25 mL of NH_4OH (30 wt% in H_2O) and 75 mL of ethanol and it is added with a rate of 0.33 mL/min. Both precipitated samples were calcined in static air at 500 °C (heating rate: 2 °C/min) for 3 h prior to their characterization.

The SAPO-34 sample has been purchased from ZR Catalyst. TG-DTA in He flow on the as-received zeolite (Fig. S1b) showed an endothermic phenomenon with the evolution of carbonaceous species (CO and, to a lower extent, CO_2), likely associated with the decomposition of residual templating agents. Hence the SAPO-34 zeolite was calcined in static air at 550 °C (heating rate: 2 °C/min) for 5 h before further characterization and testing.

Each sample was pressed into tablets and grinded and sieved to obtain a particle size between 106 and 125 μm (120–140 mesh) before catalytic tests. The In_2O_3-ZrO_2 + SAPO-34 catalyst mixture is then prepared by physically mixing the two powders prior to its loading in the reactor.

2.2. Catalyst characterization

Both the prepared In-based catalysts and the provided SAPO-34 material have been characterized by several techniques including BET, XRD, TG/DTA, SEM, CO_2- and CH_3OH-TPD, and CH_3OH-TPR.

The morphological characteristics of the samples were investigated by N_2 adsorption-desorption at 77 K to estimate the specific surface area

and pore volume of the catalysts (BET analysis), using a Micromeritics Tristar 3000 instrument. The average pore diameter was evaluated from the adsorption branch of the isotherm using the BJH method.

XRD patterns were obtained using a Panalytical Empyrean diffractometer, using a Cu-Kα radiation source.

A scanning electron microscope (SEM) (Zeiss Evo50 EP) equipped with an energy dispersive X-ray spectrometer (EDX) (Oxford Inca Energy 200 - Pentafet LZ4) was used to obtain images of the catalysts surfaces and their composition.

TPD and TPR tests were carried out at atmospheric pressure over 100 mg of catalyst loaded in a fixed-bed quartz reactor (internal diameter 0.5 cm), placed into an electric furnace. The analysis of the outlet gases was performed by a mass spectrometer (Pfeiffer Vacuum QMS200), a FT-IR spectrometer (MKS Multigas 2030) and a micro gas chromatographer (Agilent 3000). Prior to each test, the samples were heated in He flow to 500 °C (heating rate: 10 °C/min) in order to remove adsorbed water and CO_2. In a typical temperature programmed desorption (TPD) experiment, CO_2 or methanol (1% vol in He) was fed at 50 °C for 30 min, followed by 30 min of helium purge to remove weakly adsorbed species. Then, the catalyst was heated in He (constant flow rate at 100 mL/min @ 0 °C and 1 atm i.e., mL(STP)/min) up to 700 or 500 °C (heating rate 10 °C/min) in the case of CO_2-TPD or MeOH-TPD, respectively. In order to characterize the acidity of the zeolite, NH_3-TPD was performed by feeding 1% NH_3 in He at 100 °C for 1 h followed by 2 h inert purge at the same temperature and heating to 600 °C (heating rate: 10 °C/min).

Temperature Programmed Reaction (TPR) experiments were carried out in the same apparatus used for TPD experiments. The reactivity at atmospheric pressure has been investigated loading 100 mg of catalyst and flowing 1% methanol/He with a total stream of 100 mL(STP)/min over the catalyst at 50 °C. When the methanol signal detected by the mass spectrometer was stable, the temperature was increased up to 500 °C (heating rate: 10 °C/min) while monitoring the species evolving in the gas phase.

2.3. Catalyst testing

Activity measurements at high pressure were performed in a lab-scale plant equipped with a fixed-bed stainless steel reactor (internal diameter 1.1 cm) heated by an electric furnace. In a typical CO_2 to methanol (CTM) run, 2 g of In_2O_3-ZrO_2 (120–140 mesh) were loaded in the reactor. Prior to reaction, the catalyst was pre-treated at 400 °C (heating rate: 2 °C/min) overnight (16 h) under a stream containing 2000 ppm H_2 in N_2 (total flow 9 L(STP)/h). Then, temperature was decreased to 320 °C and the reactant gas mixture (H_2/CO_2 ratio equal to 3) was fed, and pressure was increased up to 38 barg at a rate of 6 barg/h.

The methanol to olefins (MTO) activity was evaluated loading 1 g of SAPO-34 and following the same pre-treatment described for the CTM run, with a constant flowrate of 3 L(STP)/h. Once the desired temperature and flowrate of H_2/CO_2 were reached, the pressure was gradually increased to 38 barg. Then, liquid methanol was fed using a Teledyne ISCO pump and vaporized in the H_2/CO_2 stream at the heated reactor inlet to obtain a concentration of 3 or 10% vol%. A regeneration procedure was performed in case of zeolite deactivation: The catalyst was cooled down in inert flow and depressurized to atmospheric pressure; then, air was fed with a total flowrate of 1.5 L(STP)/h/g and the temperature was progressively increased to 550 °C (heating rate: 0.5 °C/min), and maintained until C-containing products were observed in the gas phase (approx. 24 h).

The CO_2 to olefins (CTO) tests were performed in the same set-up and with the same procedures described for the CTM tests, but loading in this case a catalyst obtained by physically mixing 2 g of In_2O_3-ZrO_2 and 2 g of SAPO-34. In this case, the calculation of the GHSV is based on the methanol catalyst content only. Literature reports H_2/CO_2 ratio equal to 3 as the optimal value for CTO process [34], therefore this value has been used for all the runs presented in this work.

Unconverted reactants and gaseous products were analyzed using an on-line gas chromatograph (Hewlett-Packard 6890), equipped with three columns and two detectors for the analysis of C_1–C_7 hydrocarbons (Al_2O_3-plot capillary column connected to a FID), of H_2, CH_4 and CO (molecular sieve column connected to a TCD) and of CO_2 (Porapak Q column connected to the same TCD detector). In CTM and CTO tests, condensable reaction products (water and methanol) were condensed and periodically analysed by an off-line GC (HP 6890) equipped with a FID and HP-5 crosslinked 5% PH ME Siloxane capillary column. In the MTO tests, no condensation step was present prior to the analysis and therefore all the products were analysed on-line.

The results of the tests have been evaluated by estimating the CO_2 conversion and the selectivity of the various products, calculated as follows:

- CO_2 conversion

$$\chi_{CO2} = \left(1 - \frac{f_{CO2}^{out}}{f_{CO2}^{in}}\right)$$

- i-th species selectivity:

$$Selectivity_i = sel_i = \frac{f_{prod,i}^{out} \bullet nC_i}{f_{CO2}^{in} - f_{CO2}^{out}}$$

Where:

f_{CO2}^{in} and f_{CO2}^{out} are CO_2 inlet and outlet molar flowrates [mol/h].
$f_{prod,i}^{out}$ is the outlet molar flowrate of the i-th product [mol/h].
nC_i is the number of carbon atoms of the i-th species.

3. Result and discussion

3.1. Catalyst characterization

The morphological characteristics of the samples have been investigated by N_2 adsorption-desorption at 77 K to estimate the specific surface area and pore volume of the catalysts (Table 1). The coprecipitated In_2O_3-ZrO_2 catalyst shows a surface area of 96 m^2/g and an average pore volume of 0.19 cm^3/g, with an average pore diameter of 60 Å. The reference precipitated samples In_2O_3 and ZrO_2 show lower surface area of 70 and 75 m^2/g, respectively. The commercial SAPO-34 zeolite shows high surface area (769 m^2/g) and a pore volume equal to 0.31, as provided by the supplier data sheet [35].

The XRD patterns of the catalysts are shown in Fig. 1 with the corresponding reference patterns. The precipitated reference ZrO_2 and In_2O_3 samples showed the characteristic diffraction peaks of the monoclinic ZrO_2 and cubic In_2O_3 phases, respectively (Fig. 1a). In the coprecipitated In_2O_3-ZrO_2 sample the transition of ZrO_2 from the monoclinic to the tetragonal phase is observed, as reported by literature [24]. The diffraction peaks of cubic indium at $2\theta = 21°$ and 31° are also present.

The X-ray diffractograms for the SAPO-34 zeolite are reported in Fig. 1b. The sample shows a chabazite structure with major peaks at $2\theta = 9°$, 13° and 21°.

Fig. 2a shows a scanning electron microscope (SEM) image of the

Table 1
N_2 physisorption.

	A_{BET} [m^2/g]	V_{pore} [cm^3/g]	D_{pore} [Å]
In_2O_3-ZrO_2	96	0.19	60
In_2O_3	70	0.39	110
ZrO_2	75	0.13	40
SAPO-34	769 *	0.31 *	-

* From technical data sheet provided by the supplier.

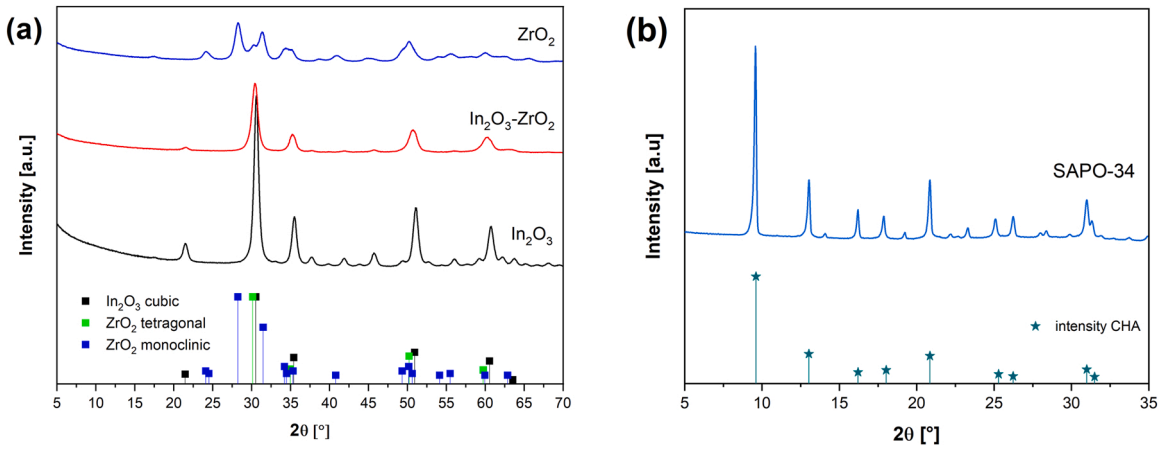

Fig. 1. XRD patterns of (a) In_2O_3-ZrO_2 coprecipitated sample compared with reference In_2O_3 and ZrO_2 precipitated samples and (b) SAPO-34 commercial sample. References (PANICSD): In_2O_3 cubic 98–016–9423, ZrO_2 tetragonal 98–017–3961, ZrO_2 monoclinic 00–007–0343, Chabazite 98–019–4279.

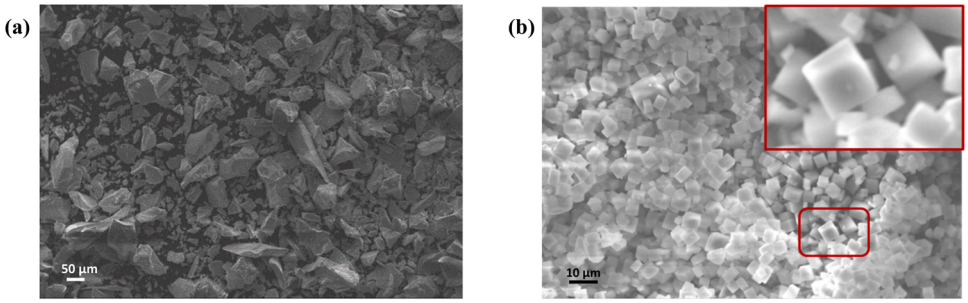

Fig. 2. SEM images of (a) In_2O_3-ZrO_2 and (b) SAPO-34 from ZR Catalyst.

coprecipitated In_2O_3-ZrO_2 catalyst. The sample appears with no regular shape and different particle size. Fig. 2b shows the SEM images of the zeolites SAPO-34 from ZR Catalyst. The crystals have a cubic shape, with an average size of 5 µm. The crystal dimension is an important parameter for the MTO performances as decreasing the crystal size has been reported as a good strategy to reduce diffusional limitations and side reactions, thus slowing down coke deposition [36].

Fig. 3 shows the results of the CO_2-TPD experiments carried out over the In_2O_3-ZrO_2 sample. The coprecipitated sample shows a significant CO_2 adsorption capacity of 41 µmol/g, with two desorption peaks centered at 150 °C and 650 °C. In particular, the high temperature evolution of CO_2 indicates that CO_2 can be strongly adsorbed on the

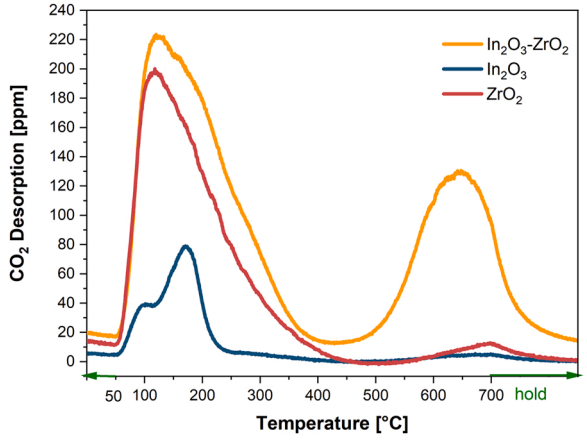

Fig. 3. Comparison of CO_2-TPD tests on In_2O_3-ZrO_2 and references In_2O_3 and ZrO_2 materials.

coprecipitated In_2O_3-ZrO_2 The reference In_2O_3 and ZrO_2 precipitated samples are also shown in Fig. 3. At variance to the coprecipitated sample, In_2O_3 and ZrO_2 show the evolution of CO_2 only at low temperature, with little to no evolution of CO_2 above 400 °C. The strong adsorption of CO_2 in the coprecipitated In_2O_3-ZrO_2 can be attributed to the increased dispersion of In, coupled to its peculiar ability to form additional vacancies as a response to structural constraints specifically imposed by the zirconia phase [24].

Fig. 4a shows the MeOH-TPD profiles obtained over the In_2O_3-ZrO_2 sample, which shows a significant methanol adsorption capacity: minor amounts of methanol (note that in Fig. 4a the methanol signal is shown multiplied by a factor 5) are desorbed unreacted in the low temperature region, below 250 °C, whereas at higher temperatures significant amounts of H_2, CO and CO_2 are observed, peaking at about 300 °C. This clearly indicates that the In_2O_3-ZrO_2 sample is able to activate methanol decomposition above 250 °C. Qualitatively similar results have been obtained over the pure precipitated materials (i.e., In_2O_3 and ZrO_2 shown in Fig. S2 of the Supplementary Material), however in these case much lower amounts of methanol have been adsorbed. Notably, the ZrO_2 sample (Fig. S2b) also shows a poor reactivity towards methanol in that the decomposition products only appear at high temperatures (above 300 °C). It is speculated that CO_2 formation in these experiments originates upon catalyst reduction; accordingly, CO_2 is not observed in the case of the zirconia catalyst due to poor reducibility of this sample. At variance, the In_2O_3 (Fig. S2a) shows a higher activity but a lower methanol adsorption capacity. These results further suggest that the In phase is well dispersed in the In_2O_3-ZrO_2 sample due to interaction with the ZrO_2 phase, since this catalyst shows high adsorption capacity and high reactivity towards methanol.

In order to decouple the amount of adsorbed methanol from the reactivity of the sample, a MeOH-TPR test was carried out by feeding 1%

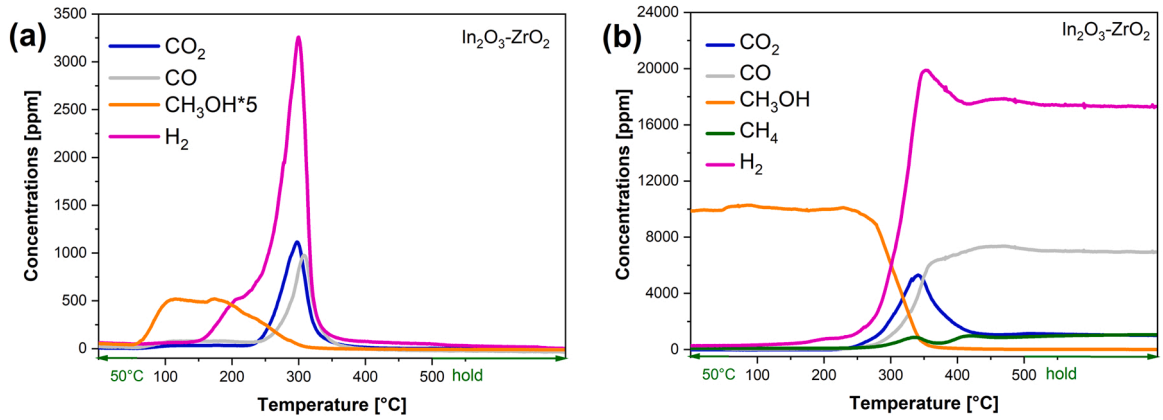

Fig. 4. (a) MeOH-TPD tests on In_2O_3-ZrO_2 and (b) MeOH-TPR on In_2O_3-ZrO_2. Experimental conditions: T = 50–500 °C, P = 0 barg, GHSV= 60 L(STP)/h/g_{cat}, MeOH 1% in He.

MeOH in He at 50 °C and progressively increasing the temperature under methanol flow. The result is shown in Fig. 4b over the coprecipitated In_2O_3-ZrO_2 catalyst. Upon increasing the temperature, methanol starts to be converted with similar temperature onset to that observed in the case of the TPD experiment, while H_2, CO_2, CO and minor amounts of CH_4 appear at the reactor outlet. CO_2 and H_2 concentrations reach a maximum at 350 °C, when methanol conversion is complete, and then decrease to reach a steady concentration at higher temperatures. When the temperature is maintained at 500 °C H_2 and CO are the main decomposition products, with lower amounts of CO_2 and CH_4. No evidence of deactivation was observed during this test on the coprecipitated sample. At variance, when the test was repeated on the pure In_2O_3 sample (Supplementary Material, Fig. S3a), CO_2 was always the main decomposition product, but when the temperature was kept at 500 °C a rapid deactivation of the sample was observed, with a significant decrease of methanol conversion. We speculate that this is because of the sintering of In_2O_3 in the case of the pure sample. In fact, while in the case of the coprecipitated sample In_2O_3 is structurally kept apart from ZrO_2, in the case of pure In_2O_3 sintering is usually indicated as the main deactivation cause [25]. Indeed, literature highlights the importance of supporting In_2O_3 on a carrier in order to achieve higher dispersion, better resistance against sintering and possibly obtain beneficial interactions with the support [21,24,25]. Among different supports, zirconia showed the best performances, leading to a material capable of outperforming bulk In_2O_3 and systems supported on alternative carriers, such as TiO_2, ZnO, SiO_2 or Al_2O_3 [25]. MeOH-TPR was also performed on the pure ZrO_2 sample (Supplementary Material, Fig. S3b): In line with the TPD data, pure ZrO_2 shows a lower reactivity Notably, in this case no CO_2 formation is observed whereas dimethyl ether (DME) is seen at the reactor outlet, originating upon methanol dehydration over the acid sites of ZrO_2.

The SAPO-34 zeolite was characterized by NH_3-TPD (Supplementary Material, Fig. S4), which resulted in a total acid site density 1.05 mmol/g with 0.68 mmol/g of basic medium sites, values well in line with literature for similar materials [36]. MeOH-TPD and TPR test have also been carried out over the SAPO-34 sample, and results are shown in Fig. 5a and b, respectively. In the case of the TPD experiment, a noticeable methanol desorption peak is seen at 90–100 °C, followed by a smaller DME peak in the range 100–250 °C. No formation of other products is observed, if one neglect small amounts of DME and olefins traces at high temperatures.

Similar results have been obtained in the case of the TPR experiment (Fig. 5b); however, in this case, due to the continuous methanol feed (not that methanol signal is divided by 10 in Fig. 5b), a much higher DME formation is observed between 100 and 350 °C. The maximum concentration reached by DME is about equal to 3700 ppm at 270 °C. At higher temperature, DME is consumed, and olefins concentration (mostly propylene and ethylene) starts to increase. The observed results are well in line with mechanistic indications on DME as key intermediate in olefins production [37]. Olefins evolution in the gas phase reaches a maximum before 400 °C, and decreases at higher temperatures, while methanol decomposition products such as CO and H_2 increase in the effluents. When the temperature is kept at 500 °C, methanol decomposition products as well as olefin continue to decrease, indicating the progressive deactivation of the zeolite, likely due to the accumulation of carbonaceous species on the catalyst [38]. Notably, CH_4 evolution is

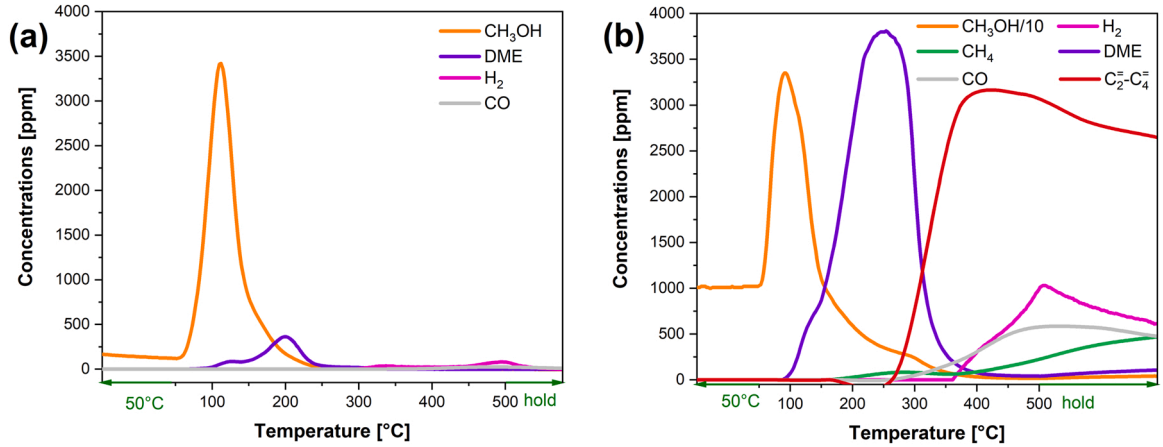

Fig. 5. (a) MeOH-TPD and (b) MeOH-TPR on SAPO-34 zeolite. Experimental conditions: T = 50–500 °C, P = 0 barg, GHSV= 60 L(STP)/h/g_{cat}, MeOH 1% in He.

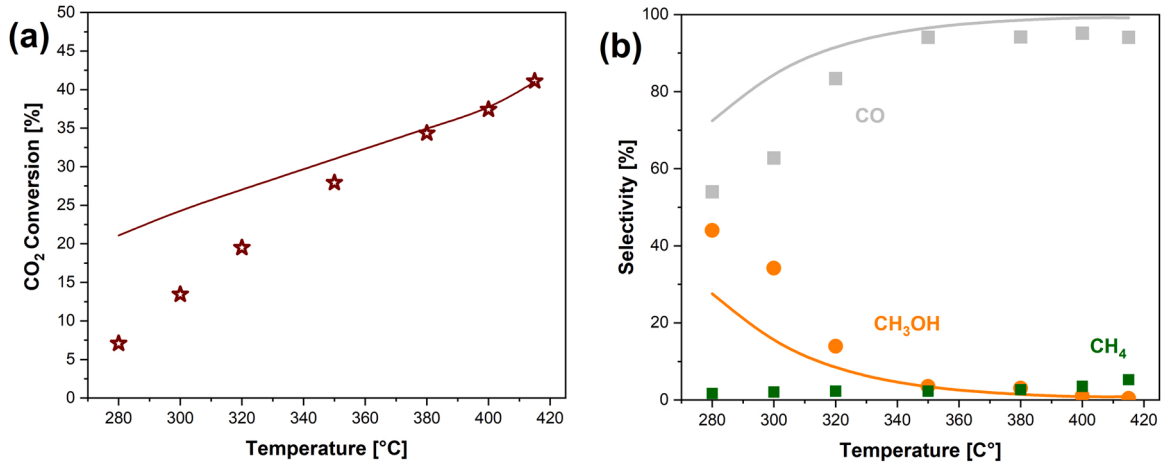

Fig. 6. Reactivity of In_2O_3-ZrO_2 in the CO_2 to methanol synthesis: (a) CO_2 conversion and (b) products selectivity. The results are compared with thermodynamic equilibrium data. Experimental conditions: T = 280–400 °C, P = 38 bar, GHSV= 3 L(STP)/h/ g_{cat}, H_2/CO_2 = 3.

observed at high temperature, with increasing concentration as the zeolite deactivation proceeds. At temperatures higher than 350 °C, CO and CH_4 are also formed. Accordingly, these data indicate that the selected ZR SAPO-34 zeolite is active in the methanol-to-olefins reaction.

3.2. CO_2 to methanol (CTM) testing on In_2O_3-ZrO_2

The In_2O_3-ZrO_2 sample was then tested in the methanol synthesis from CO_2 in the high-pressure setup. In these tests, the effect of temperature has been addressed. 2 g of catalyst were loaded in the reactor tested in the temperature range 280–415 °C, keeping constant pressure (38 barg) and space velocity (3 L(STP)/h/g_{cat}). The choice of this relatively high temperature and low pressure for methanol synthesis aimed at replicating the experimental conditions of the CO_2 to olefins (CTO) process, which requires intermediate pressures (10–40 bar) and relatively high temperatures (350–400 °C) [39]. Heat and mass transport limitations were ruled out using empirical criteria.

Fig. 6 shows the results obtained on the In_2O_3-ZrO_2 catalyst. in terms of selectivity and CO_2 conversion vs. temperature. The results are compared with thermodynamic equilibrium data (solid lines), evaluated considering the methanol synthesis reaction and the RWGS reaction. The experimental data are calculated as average of the stationary values for each condition.

At low temperature, conversion is lower than equilibrium; methanol and CO are the most abundant products, with minor amounts of CH_4. Conversion and products selectivity approach equilibrium values at high temperatures (380–400 °C), corresponding to a CO_2 conversion of about 35% and a methanol selectivity less than 5%, as thermodynamics largely favour CO formation in these conditions. CH_4 concentration increases at high temperature, likely as the result of the methanation of CO and/or CO_2, which is also thermodynamically favoured in these conditions.

The same CTM test summarized in Fig. 6 is shown in Fig. 7 as a function of the Time on Stream (ToS). Note that while CO and CH_4 are the result of the on-line analysis, methanol productivity is assessed by periodically removing and analysing the condensed liquid products, and it is hence reported as average value for the corresponding ToS. CO_2 conversion and product selectivity indicate the substantial stability of the coprecipitated sample until 400 °C. At 415 °C the sample shows increasing conversion over time, with an increase of CH_4 at the expenses of CO production. After about 100 h the temperature was brought back to 320 °C in order compare the catalyst performance before and after the high temperature condition. The results show that no significant changes occur both in CO_2 conversion and product selectivity (compare data at ToS 150 h and 350 h in Fig. 7), pointing out the substantial catalyst stability for prolonged ToS even at high temperatures.

3.3. Methanol-to-olefins (MTO) on SAPO-34

The reactivity of the selected zeolite sample has also been investigated in the MTO reactivity, simulating the experimental conditions that the zeolite is expected to operate in the CO_2 to olefins process i.e., low concentrations of methanol in the presence of CO_2 and H_2, and high pressure (while the conventional MTO process is performed at maximum 5 barg).

Fig. 8 shows the results obtained as a function of ToS of a run carried out at 380 °C, 38 barg and 10% in 90% of H_2/CO_2 in terms of flowrates of the products leaving the reactor. At variance with the CTM run, in this case diffusional limitations cannot be ruled out using empirical criteria due to the difficult estimation of a reaction rate for methanol decomposition. During the initial 6 h, no methanol is detected at the outlet, indicating its complete conversion. Methanol is converted to paraffins with a selectivity of nearly 90% at ToS = 3 h. Then, paraffins start to decrease while olefins increase as methanol starts to be detected at the outlet. At ToS = 8 h also the olefins decrease, as DME starts to be detected while methanol concentration at the outlet keeps increasing, indicating the deactivation of the zeolite, likely caused by the formation of C deposits [30].

The paraffin selectivity in conventional MTO (i.e., at high T and low P) is normally attributed to the H_2 transfer reaction [40], leading to the formation of aromatic species. However, in the presence of high H_2 partial pressures the hydrogen transfer reaction should be to some extent inhibited [33]. In these conditions, an additional paraffins formation pathway may be attributed to the successive hydrogenation of the formed olefins on the Bronsted acid sites of the bare zeolite [41]. In fact, the effluents order observed in Fig. 8 (paraffins-olefins-DME) as the zeolite progressively deactivates could be in line with the reduction of contact time between the reacting stream and the zeolite. In this way, assuming that C deposits are progressively masking the zeolite active sites as the contact time is reduced the selectivity towards intermediate species increase, and as DME is an intermediate in olefin formation (as well observed from MeOH-TPR in Fig. 5b), olefins are likely intermediates in paraffins formation. It remains unclear to what extent olefins arise from the sole hydrogen transfer reactions or from the direct hydrogenation of the corresponding olefins. When an MTO test was attempted on a fresh SAPO-34 to clarify this aspect in the same experimental conditions but with N_2 instead of the H_2/CO_2 mixture, the zeolite deactivated in less than 1 h, preventing the collection of meaningful selectivity data.

The conversion of CO_2 remained below 5% during the whole duration of the test. CH_4 production starts as soon as methanol is fed and seems unaffected by the progressive deactivation of the zeolite, with a selectivity reaching 15% after about 10 h on stream.

After the run, the zeolite was regenerated by oxidation and again tested in the MTO reaction under the same conditions as in Fig. 8, but with a lower methanol concentration (3% CH_3OH in H_2/CO_2 3/1 mol/mol). The zeolite was found to be stable for more than 50 h under such conditions, thus suggesting that decreasing the methanol concentration can effectively lengthen the zeolite catalyst lifetime.

The effect of temperature on the zeolite stability has been investigated, testing the zeolite (with 10% methanol) at 400 and 425 °C. At variance with the data collected at 380 °C, the ZR zeolite showed stable product selectivity with complete methanol conversion for more than 300 h on stream for each temperature. Notably, when the temperature was then lowered under the same conditions at 380 °C, the zeolite deactivated again in about 5 h, with the same behavior observed in Fig. 8. The stable behavior of the SAPO-34 zeolite at high temperature can be ascribed to the occurrence of hydrogenation reactions that slow down the carbon deposition, due the high partial pressure of H_2 and H_2O in the reaction environment[33]. Indeed, literature indicates that the Bronsted acid sites of SAPO-34 can hydrogenate the aromatic deposits as well as the olefins leading to their formation, resulting in a much lower deactivation rate at the expenses of a lower O/P ratio [33,41]. Fig. 9 shows the product distribution and the conversion of CO_2 and methanol at the temperatures of 400 and 425 °C, where stable performances were obtained.

In fact, while the conversion of methanol remains complete at both temperatures and the conversion of CO_2 stays at comparable levels (13% and 11% at 400 and 425 °C, respectively), increasing the temperature to 425 °C causes relevant decrease in olefins selectivity, that drops from 23% to 2% with a corresponding increase in paraffin (olefin/paraffin ratio from 0.45 to 0.04) and CH_4 selectivity. This could be attributed to the faster hydrogenation kinetics at higher temperature, further increasing the production of paraffins and methane, with the latter nearly doubling its concentration between the two temperatures Other than the global olefin/paraffin ratio, also the molecular weight of the products shifts towards lower values, with increasing amount of C_2 and C_3 products at the expenses of C_4.

In similar fashion, the effect of the GHSV was also investigated at the pressures of 38 barg at the fixed temperature of 425 °C, and the results are reported in Fig. 10. The selectivity and conversion values represent stationary conditions averaged in at least 30 h, as the system did not show sign of deactivation at the investigated process conditions.

Starting from the point we have previously discussed at 38 barg, 425 °C and 3 L(STP)/h/g, increasing the space velocity up to 9 L(STP)/h/g, CO_2 conversion progressively decreases from 11% to 5% with a simultaneous decrease of the CO and CH_4 selectivity. Methanol concentration in the effluents remain null at 6 L(STP)/h/g indicating complete conversion, but small amounts start to be detected when the GHSV is increased to 9 L(STP)/h/g (methanol conversion = 99.8%). When increasing the GHSV at constant temperature and pressure the olefin selectivity increases at the expense of paraffins (and CH_4), reaching 36% selectivity at 9 L(STP)/h/g and 38 barg, corresponding to an olefin/paraffin ratio of 0.85. The GHSV effect is consistent with the sequential hydrogenation of the olefins produced by MTO reactivity in the zeolite. In fact, by reducing the contact time, the intermediate species (i.e., the olefin) is favored with respect to final hydrogenated product (i.e., the paraffin).

Accordingly, the test of the zeolite reactivity in the MTO reaction under conditions of practical relevance for the CO_2 to olefins process, pointed out that the zeolite can be operated under stable conditions when the methanol partial pressure is sufficiently low and temperatures high enough in the presence of high H_2 partial pressures. However, it is also worth noticing that these conditions favor the hydrogenation capacity of the system, leading to the hydrogenation of the formed olefins to paraffins, thus lowering the overall olefin/paraffin ratio.

3.4. CO_2-to-olefins (CTO) testing on mixture In_2O_3-ZrO_2 + SAPO-34

The one-pot CO_2 to olefins methanol-mediated process was tested by physically mixing the two catalytic materials in a 1:1 ratio by weight (2 g coprecipitated In_2O_3-ZrO_2 + 2 g SAPO-34). The two reactions occur in series, since the MTO step converts methanol formed in the first step

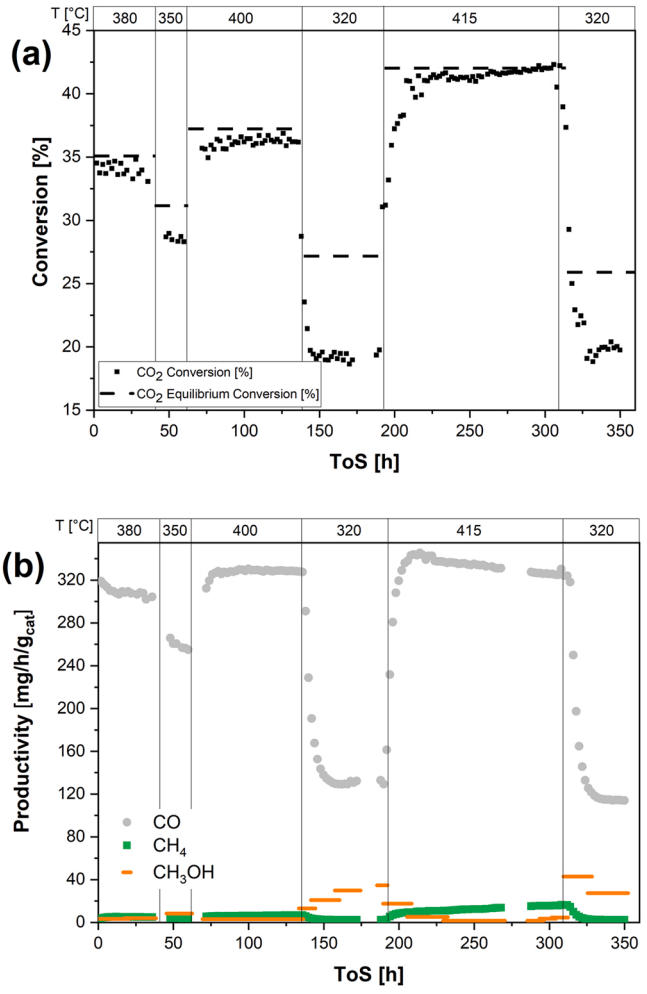

Fig. 7. In_2O_3-ZrO_2 run test for stability (a) CO_2 conversion and (b) Productivity. Experimental conditions: T = 320–415 °C, P = 38 barg, GHSV= 3 L(STP)/h/g_{cat}, H_2/CO_2 = 3.

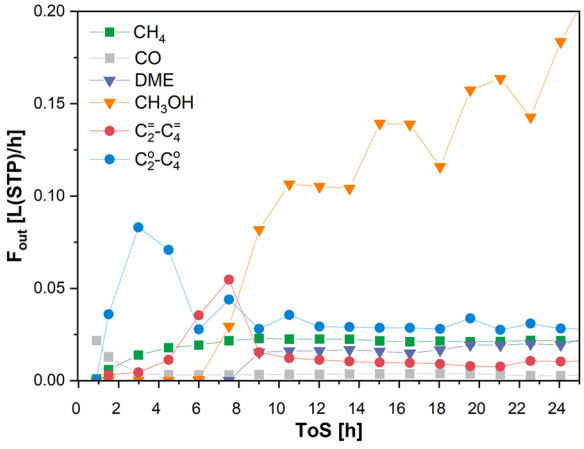

Fig. 8. MTO run with SAPO-34 (ZR catalyst): outlet flowrate (CO_2 and H_2 not shown) as a function of ToS. Experimental conditions: T = 380 °C, P = 38 barg, GHSV= 3 L(STP)/h/g, 10% MeOH in H_2/CO_2 = 3.

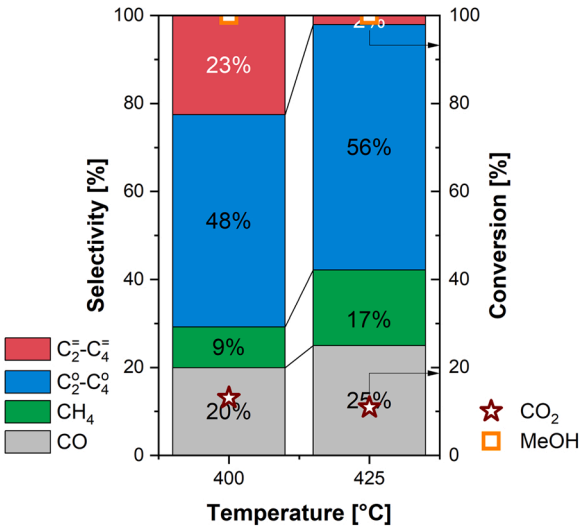

Fig. 9. Temperature effect on the SAPO-34 catalyst. Experimental conditions: P = 38 barg, GHSV= 3 L(STP)/h/g, 10% MeOH in $H_2/CO_2 = 3$.

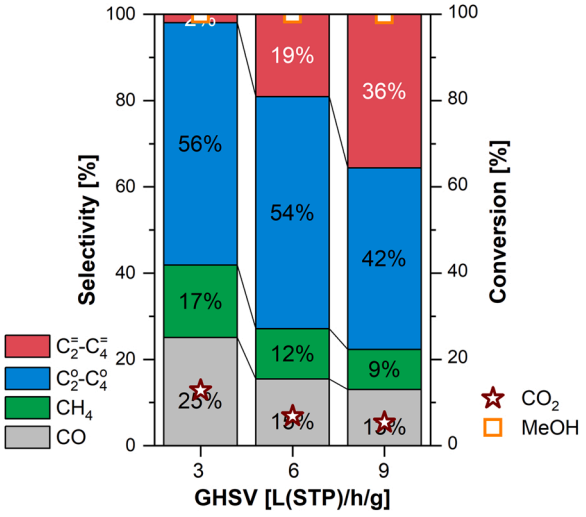

Fig. 10. GHSV effect on the ZR SAPO-34 catalyst. Experimental conditions: T = 425 °C, GHSV= 3–9 L(STP)/h/g, 10% MeOH in $H_2/CO_2 = 3$.

of CO_2 hydrogenation (CTM). On these bases, the second reaction is expected to shift the equilibrium of the first by consuming all the produced methanol. However, the formation of water may limit this effect. In fact, water is a product of both CTM and MTO reactions, and the water produced by the latter will hinder the former, possibly compensating for the positive effect of methanol removal.

The results obtained at different temperatures in the CO_2 to olefins process with the mixture In_2O_3-ZrO_2 + SAPO-34 catalyst are shown in Fig. 11. It can be observed that CO_2 conversion increases with temperature and approaches equilibrium at temperatures higher than 380 °C, as observed in the CTM run on In_2O_3-ZrO_2.

Regarding the products selectivity, CO is always the most abundant product. Methanol and DME are observed in significant amounts below 350 °C, since at low temperatures the MTO process is not active and, as a result, unconverted methanol and DME are present in the products stream. CO selectivity reaches its maximum at 350 °C, a temperature that is high for methanol synthesis and low for MTO; C_2-C_4 olefins and paraffins production is observed at temperature higher than 350 °C, when the C-C coupling from methanol over zeolites is kinetically favourable [37,42]. CO selectivity reaches its minimum value of about 60% at 380 °C, where a maximum in C_2-C_4 olefin selectivity is also observed, corresponding to 18.5%, C-based and to 46% CO-free, with an olefin/paraffin ratio of about 1. Although literature often reports higher CO-free selectivity for lower olefins during CTO runs on similar catalytic systems, such results are usually obtained at lower pressure. This usually results in higher O/P ratios, at the expenses of higher CO selectivity and lower CO_2 conversion [34,39]. At variance, working at 38 barg allows us to increase CO_2 conversion up to equilibrium levels and to favor methanol formation in the first step, resulting in lower CO selectivity. Overall, the lower olefins yield obtained in this work at 380 °C in the experimental conditions reported in Fig. 11 is equal to 6.6%, which is in the high range of the literature yield spectrum, comprised between 4% and 7% [21,34,43]).

Between 380 and 400 °C olefins start to decrease while the paraffins slowly increase to a plateau. This effect can be explained with the role of secondary hydrogenation reactions, which lead to the formation of paraffins and have been observed even on the bare zeolite during MTO tests, and could occur also over In_2O_3-ZrO_2 in the presence of H_2. For temperatures higher than 400 °C, both olefins and paraffins decrease while CO and CH_4 increase. Because of the lower methanol equilibrium yield, determining the steep increase in CO selectivity and the lower selectivity to C_{2+} products.

By comparing the results obtained in the CTO run (Fig. 11) with the results obtained in the CTM run (Fig. 6), we observe comparable CO_2 conversion at high temperature (380–415 °C), that well matches the thermodynamic equilibrium. This means that the sequence of the two steps is not able to increase the overall CO_2 conversion, likely because of the water produced in the second step of the process. But, on the other hand, a beneficial effect on product selectivity observed. Indeed, CO selectivity is roughly 60% at 380°C during the CTO test on the In_2O_3-ZrO_2 + SAPO-34 mechanical mixture, while in corresponding conditions of the CTM run on In_2O_3-ZrO_2 alone it reached 94% (see Fig. 6b). At the same time, the C-selectivity towards C_2-C_4 hydrocarbons reaches values close to 40%, which is considerably higher than the corresponding methanol selectivity observed in the absence of the zeolite (around 5% at 380 °C, see Fig. 6b).

CO_2 hydrogenation via a methanol-mediated route over bifunctional catalysts is a burdensome process in terms of catalysts stability: the high H_2O partial pressure – increased with respect to the corresponding process using CO as C feedstock – may worsen the catalyst performance over time; [16,44]; in addition, the MTO zeolite is subject to carbon deposition [45] and the interaction between the CTM and MTO catalysts may result in the cross contamination of the samples [34]. On these bases, the stability of the mixed In_2O_3-ZrO_2 + SAPO-34 mechanical mixture with ToS under different conditions has been analyzed, and results are shown in Fig. 12.

Notably, replicated runs have been carried out at 380 and 400 °C, and hence the stability of the catalyst can be evaluated. As shown in Fig. 12, deactivation was observed, very likely at the expenses of the In_2O_3-ZrO_2 sample in view of the increase of the CO production and of the observation that the zeolite was rather stable at high temperatures and/or in the presence of small methanol concentration. In fact, in the MTO tests previously discussed the zeolites showed high stability in the system containing low concentration of methanol, which is the case in the combined process. Notably, while the role of hydrogen in lowering the zeolite deactivation due to coking and increasing the catalyst life is established [33], the role of the relevant amounts of the formed CO on the zeolite lifetime is more controversial. It has been reported that co-feeding high-pressure CO in a MTO process can in fact results in changes in catalyst lifetime and products selectivity [46]. However, its mechanistic role has not been defined and its effect deeply depends on the partial pressure in the system, leading to different effects observed [46]. Nonetheless, Chen et al. [47] reported an increase in aromatics formation associated with high partial pressure of CO, that can contextually lead to lower stability of the system.

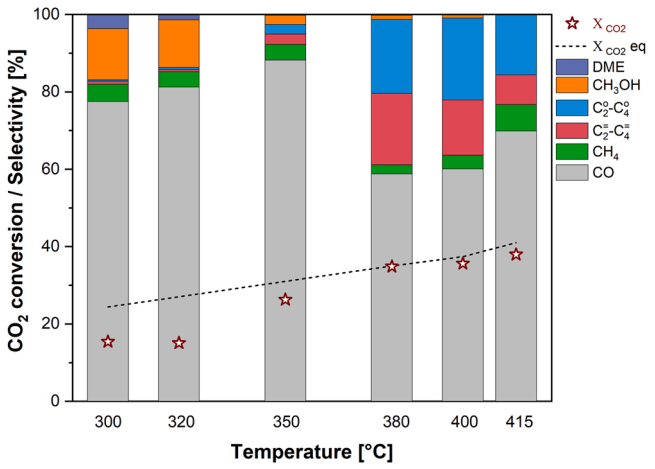

Fig. 11. Effect of temperature on In_2O_3-ZrO_2 +SAPO-34 ZR (1:1 wt ratio). Experimental conditions: T = 300–415 °C, P = 38 bar, GHSV= 3 L(STP)/h/g_{cat}, H_2/CO_2 = 3.

3.5. *One-pot olefins production via modified Fischer-Tropsch (MFT) and methanol-mediated routes*

It is of interest to make a direct comparison of the results in the synthesis of olefins through the MFT pathway (investigated in a previous work by some of us, [3]) and the MeOH-mediated route (this work).

It is worth noticing that the operating conditions of the two processes are very different, with the exception of the low space velocity (2.7 vs 3 L(STP)/h/g_{cat} for MFT and MeOH-mediated, respectively). The MFT route is operated with a single Fe-based material able to catalyse both RWGS and FT reactions under milder conditions of temperature (270 vs 380 °C) and pressure 270 °C and 5 barg) with respect to the MeOH-mediated route (380 °C and 38 barg). In particular, the higher pressure and temperatures used in the methanol-mediated route are dictated by the co-presence of methanol synthesis catalyst and the zeolite, respectively. Indeed, high pressures are required to push the methanol synthesis, whereas high temperatures are necessary to activate the SAPO-34 zeolite in the MTO process, although this limit thermodynamically the CO_2 conversion to methanol. It is worth noticing that a physical mixture of the two CTM and MTO catalysts has been used in this work, but it is well known how proximity of the active phases is a key parameter for the process optimization. For this reason, ongoing work is focusing on the effects of different integration manners and supported catalytic systems.

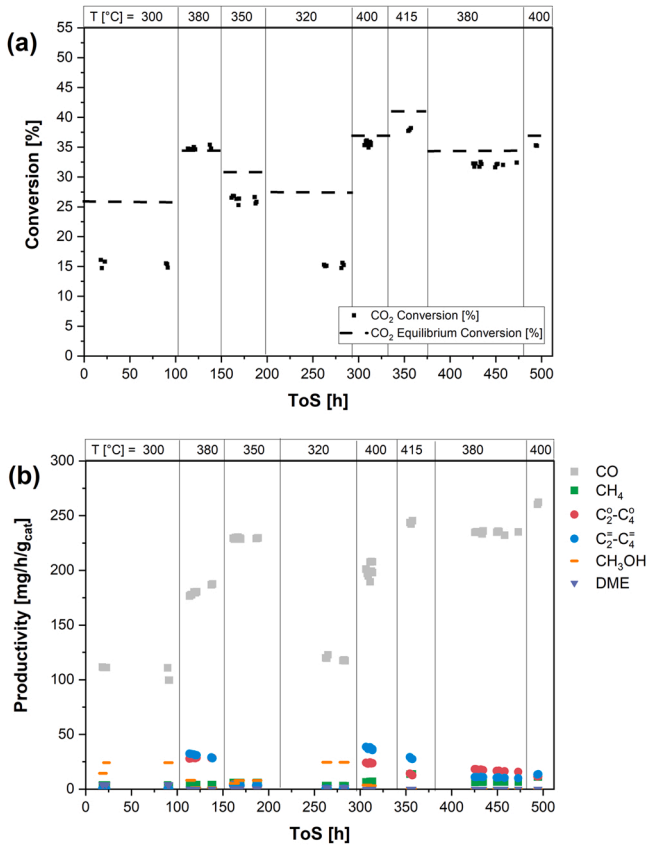

Fig. 12. Effect of ToS and deactivation (a) CO_2 conversion and (b) productivity. Experimental conditions: T = 300–415 °C, P = 38 bar, GHSV= 3 L(STP)/h/g_{cat}, H_2/CO_2 = 3.

The results obtained with the two CTO routes are shown in terms of CO_2 conversion and selectivity in Fig. 13 (CO-free and total C-selectivity in Fig. 13a and b, respectively). From Fig. 13a we can observe that CO_2 conversion is very similar despite the different processes, catalysts and operating conditions: 38% for the MTF and 35% for the MeOH-mediated routes. Both processes are comprised by two consecutive steps: RWGS and FT in the case of MFT and CTM and MTO in the case of the MeOH-mediated route. Notably, in both cases the second reaction is not thermodynamically limited and produces significant amounts of water, which is also a product of the thermodynamically limited first reaction, thus limiting the beneficial effect of the one-pot synthesis in terms of overall CO_2 conversion. Therefore, both MFT and MeOH-mediated processes are expected to be operated in the presence of a significant recycle after the product separation.

Considering the product distribution, the CO-free selectivity toward lower olefins is comparable between the two pathways (43% vs 46%, red bars in Fig. 13a), while relevant differences can be observed in the by-products (Fig. 13b): the MFT route produces less paraffins (O/P = 5), but the products follow the Anderson-Schulz-Flory (ASF) distribution, and therefore relevant amounts of CH_4 and heavier hydrocarbons (C_5^+) are present; in the MeOH-mediated process the O/P ratio is lower, and methanol formation is limited by thermodynamics, resulting in CO (both from RWGS and methanol decomposition) as main product in terms of overall C-selectivity.

For these reasons, despite the similarities regarding CO_2 conversion, the challenges that the two processes have to face are different: in the case of MFT route, C_5^+ hydrocarbons and especially CH_4 need to be reduced, while in MeOH-mediated pathway CO formation must be

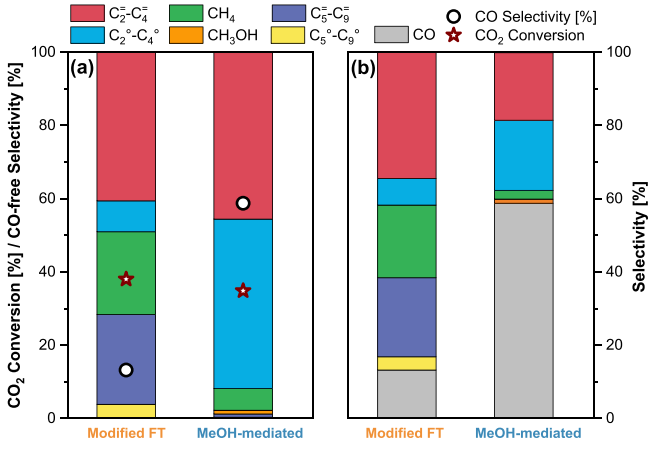

Fig. 13. Comparison of different routes for light olefins synthesis from CO_2 in terms of (a) of CO_2 conversion/CO-free selectivity and (b) selectivity. Experimental conditions modified FT: T = 270 °C, P = 5 barg, GHSV= 2.7 L(STP)/h/g_{cat}, H_2/CO_2 = 3. Experimental conditions MeOH-mediated: T = 380 °C, P = 38 barg, GHSV= 3 L(STP)/h/g_{cat}, H_2/CO_2 = 3.

decreased. However, unlike methane, CO is active in methanol synthesis and therefore, it is possible to design a process with recirculation of CO, to increase the carbon efficiency of this process.

4. Conclusions

The reactivity of bifunctional catalysts able to directly hydrogenate CO_2 into C_2-C_4 light olefins is investigated in this work. The bifunctional catalytic systems, that operate according to the so-called methanol-mediated route, combine a catalyst for the CO_2 hydrogenation to methanol (CTM catalyst) and a catalyst for the methanol conversion to olefins (MTO catalyst).

To better understand the interaction of the two catalytic materials, the reactivity of the individual catalysts has also been studied in the conditions of the overall CO_2 to olefins process (CTO), i.e., in the presence of H_2/CO_2 streams at high pressures and high temperatures. A coprecipitated In_2O_3-ZrO_2 catalyst was selected as CTM catalyst. This material showed good stability even at high temperatures, although thermodynamics limit methanol selectivity in favor of CO in such conditions. A commercial SAPO-34 zeolite was used to catalyze the MTO reaction. When tested under high H_2 partial pressures, the zeolite showed increased paraffin selectivity with respect to conventional MTO performances. However, the presence of H_2 increased the zeolite stability, significantly slowing down the deactivation induced by coking.

The bifunctional catalyst for the one-pot synthesis of lower olefins was obtained physically mixing in a 1:1 wt ratio the In_2O_3-ZrO_2 and SAPO-34 catalytic materials. This catalytic system was effective in the direct synthesis of olefins from CO_2 at high pressure and temperature. These operating conditions are dictated by the methanol synthesis catalyst and the reactivity of the zeolite, respectively, since high pressures are required to push the methanol synthesis, whereas high temperatures are necessary to activate the SAPO-34 zeolite in the MTO process, although this limit thermodynamically the CO_2 conversion to methanol. Accordingly, a trade-off in the selection of the operating conditions is required. At 380 °C, 38 barg and 3 L(STP)/h/g_{cat} the CO_2 conversion is around 35% and the olefins yield around 7%, being the C_2-C_4 olefins selectivity around 50% on a CO-free basis. CO and CH_4 selectivities are 60% and less than 5%, respectively. Higher temperatures increase CO and CH_4 selectivity.

A comparison of the catalytic performance and characteristics of the methanol-mediated route with the modified Fischer-Tropsch pathway point out the different performances of the two catalytic systems: CO reduction is the challenge of the methanol-mediated route while CH_4 and C_5^+ hydrocarbons formation is the challenge of the MFT reaction.

CRediT authorship contribution statement

C. Coffano: Investigation, Writing - original draft, Visualization, Validation. **A. Porta**: Investigation, Writing – review & editing, Methodology, Validation. **C.G. Visconti**: Conceptualization, Supervision, Funding acquisition. **F. Rabino**: Methodology, Formal analysis. **G. Franzoni**: Methodology, Project administration. **B. Picutti**: Formal analysis, Funding acquisition. **L. Lietti**: Supervision, Funding acquisition, Writing – review & editing.

Declaration of Competing Interest

The authors declare that they have no known competing financial interests or personal relationships that could have appeared to influence the work reported in this paper.

Data availability

Data will be made available on request.

Appendix A. Supporting information

Supplementary data associated with this article can be found in the online version at doi:10.1016/j.cattod.2023.114133.

References

[1] J. Gibbins, H. Chalmers, Carbon capture and storage, Energy Policy 36 (2008) 4317–4322, https://doi.org/10.1016/j.enpol.2008.09.058.
[2] A. Corma, F.V. Melo, L. Sauvanaud, F. Ortega, Light cracked naphtha processing: Controlling chemistry for maximum propylene production, Catal. Today 107–108 (2005) 699–706, https://doi.org/10.1016/j.cattod.2005.07.109.
[3] C.G. Visconti, M. Martinelli, L. Falbo, et al., CO_2 hydrogenation to lower olefins on a high surface area K-promoted bulk Fe-catalyst, Appl. Catal. B Environ. 200 (2017) 530–542, https://doi.org/10.1016/j.apcatb.2016.07.047.
[4] T. Numpilai, T. Witoon, N. Chanlek, et al., Structure–activity relationships of Fe-Co/K-Al2O3 catalysts calcined at different temperatures for CO_2 hydrogenation to light olefins, Appl. Catal. A Gen. 547 (2017) 219–229, https://doi.org/10.1016/j.apcata.2017.09.006.
[5] T. Wu, J. Lin, Y. Cheng, et al., Porous Graphene-Confined Fe-K as Highly Efficient Catalyst for CO_2 Direct Hydrogenation to Light Olefins, ACS Appl. Mater. Interfaces 10 (2018) 23439–23443, https://doi.org/10.1021/acsami.8b05411.
[6] I.A. da Silva, C.J.A. Mota, Conversion of CO_2 to light olefins over iron-based catalysts supported on niobium oxide, Front Energy Res 7 (2019) 1–8, https://doi.org/10.3389/fenrg.2019.00049.
[7] M.K. Gnanamani, H.H. Hamdeh, W.D. Shafer, et al., Fischer-tropsch synthesis: Effect of potassium on activity and selectivity for oxide and carbide fe catalysts, Catal. Lett. 143 (2013) 1123–1131, https://doi.org/10.1007/s10562-013-1110-7.
[8] Z. Li, W. Wu, M. Wang, et al., Ambient-pressure hydrogenation of CO_2 into long-chain olefins, Nat. Commun. (2022) 13, https://doi.org/10.1038/s41467-022-29971-5.
[9] M. Ronda-Lloret, G. Rothenberg, N.R. Shiju, A critical look at direct catalytic hydrogenation of carbon dioxide to olefins, ChemSusChem 12 (2019) 3896–3914, https://doi.org/10.1002/cssc.201900915.
[10] D. Gao, W. Li, H. Wang, et al., Heterogeneous catalysis for CO_2 conversion into chemicals and fuels, Trans. Tianjin Univ. 28 (2022) 245–264, https://doi.org/10.1007/s12209-022-00326-x.
[11] D. Wang, Z. Xie, M.D. Porosoff, J.G. Chen, Recent advances in carbon dioxide hydrogenation to produce olefins and aromatics, Chem 7 (2021) 2277–2311, https://doi.org/10.1016/j.chempr.2021.02.024.
[12] T. Numpilai, C.K. Cheng, J. Limtrakul, T. Witoon, Recent advances in light olefins production from catalytic hydrogenation of carbon dioxide, Process Saf. Environ. Prot. 151 (2021) 401–427, https://doi.org/10.1016/j.psep.2021.05.025.
[13] J. Chen, X. Wang, D. Wu, et al., Hydrogenation of CO_2 to light olefins on CuZnZr@(Zn-)SAPO-34 catalysts: Strategy for product distribution, Fuel 239 (2019) 44–52, https://doi.org/10.1016/j.fuel.2018.10.148.
[14] R.P. Ye, J. Ding, W. Gong, et al., CO_2 hydrogenation to high-value products via heterogeneous catalysis, Nat. Commun. (2019) 10, https://doi.org/10.1038/s41467-019-13638-9.
[15] P. Wang, F. Zha, L. Yao, Y. Chang, Synthesis of light olefins from CO_2 hydrogenation over (CuO-ZnO)-kaolin/SAPO-34 molecular sieves, Appl. Clay Sci. 163 (2018) 249–256, https://doi.org/10.1016/j.clay.2018.06.038.
[16] Z. Li, J. Wang, Y. Qu, et al., Highly selective conversion of carbon dioxide to lower olefins, ACS Catal. 7 (2017) 8544–8548, https://doi.org/10.1021/acscatal.7b03251.
[17] J. Wang, A. Zhang, X. Jiang, et al., Highly selective conversion of CO_2 to lower hydrocarbons (C2-C4) over bifunctional catalysts composed of In2O3-ZrO2 and zeolite, J. CO_2 Util. 27 (2018) 81–88, https://doi.org/10.1016/j.jcou.2018.07.006.
[18] P. Ticali, D. Salusso, R. Ahmad, et al., CO2hydrogenation to methanol and hydrocarbons over bifunctional Zn-doped ZrO2/zeolite catalysts, Catal. Sci. Technol. 11 (2021) 1249–1268, https://doi.org/10.1039/d0cy01550d.
[19] L. Tan, P. Zhang, Y. Cui, et al., Direct CO_2 hydrogenation to light olefins by suppressing CO by-product formation, Fuel Process Technol. 196 (2019), 106174, https://doi.org/10.1016/j.fuproc.2019.106174.
[20] J. Gao, C. Jia, B. Liu, Direct and selective hydrogenation of CO_2 to ethylene and propene by bifunctional catalysts, Catal. Sci. Technol. 7 (2017) 5602–5607, https://doi.org/10.1039/c7cy01549f.
[21] S. Dang, P. Gao, Z. Liu, et al., Role of zirconium in direct CO_2 hydrogenation to lower olefins on oxide/zeolite bifunctional catalysts, J. Catal. 364 (2018) 382–393, https://doi.org/10.1016/j.jcat.2018.06.010.
[22] T. Numpilai, S. Kahadit, T. Witoon, et al., CO_2 Hydrogenation to Light Olefins Over In2O3/SAPO-34 and Fe-Co/K-Al2O3 Composite Catalyst, Top. Catal. 64 (2021) 316–327, https://doi.org/10.1007/s11244-021-01412-5.
[23] M.S. Frei, C. Mondelli, R. García-Muelas, et al., Atomic-scale engineering of indium oxide promotion by palladium for methanol production via CO_2 hydrogenation, Nat. Commun. 10 (2019) 1–11, https://doi.org/10.1038/s41467-019-11349-9.
[24] M.S. Frei, C. Mondelli, A. Cesarini, et al., Role of Zirconia in Indium Oxide-Catalyzed CO_2 Hydrogenation to Methanol, ACS Catal. 10 (2020) 1133–1145, https://doi.org/10.1021/acscatal.9b03305.
[25] O. Martin, A.J. Martín, C. Mondelli, et al., Indium oxide as a superior catalyst for methanol synthesis by CO2hydrogenation, in: Angew Chemie - Int Ed, 55, 2016, pp. 6261–6265, https://doi.org/10.1002/anie.201600943.

[26] J. Gao, C. Jia, B. Liu, Direct and selective hydrogenation of CO_2 to ethylene and propene by bifunctional catalysts, Catal. Sci. Technol. 7 (2017) 5602–5607, https://doi.org/10.1039/c7cy01549f.
[27] H. Tian, J. Yao, F. Zha, et al., Catalytic activity of SAPO-34 molecular sieves prepared by using palygorskite in the synthesis of light olefins via CO_2 hydrogenation, Appl. Clay Sci. 184 (2020), 105392, https://doi.org/10.1016/j.clay.2019.105392.
[28] Q. Sun, Z. Xie, J. Yu, The state-of-the-art synthetic strategies for SAPO-34 zeolite catalysts in methanol-to-olefin conversion, Natl. Sci. Rev. 5 (2018) 542–558, https://doi.org/10.1093/nsr/nwx103.
[29] A. Ramirez, A. Dutta Chowdhury, A. Dokania, et al., Effect of Zeolite Topology and Reactor Configuration on the Direct Conversion of CO_2 to Light Olefins and Aromatics, ACS Catal. 9 (2019) 6320–6334, https://doi.org/10.1021/acscatal.9b01466.
[30] P. Tian, Y. Wei, M. Ye, Z. Liu, Methanol to Olefins (MTO): From Fundamentals to Commercialization, ACS Catal. 5 (2015) 1922–1938, https://doi.org/10.1021/acscatal.5b00007.
[31] S. Xu, Y. Zhi, J. Han, et al.. Advances in Catalysis for Methanol-to-Olefins Conversion, 1st ed..,, Elsevier Inc,, 2017.
[32] A. Dokania, A. Dutta Chowdhury, A. Ramirez, et al., Acidity modification of ZSM-5 for enhanced production of light olefins from CO_2, J. Catal. 381 (2020) 347–354, https://doi.org/10.1016/j.jcat.2019.11.015.
[33] X. Zhao, J. Li, P. Tian, et al., Achieving a Superlong Lifetime in the Zeolite-Catalyzed MTO Reaction under High Pressure: Synergistic Effect of Hydrogen and Water, ACS Catal. 9 (2019) 3017–3025, https://doi.org/10.1021/acscatal.8b04402.
[34] P. Gao, S. Dang, S. Li, et al., Direct Production of Lower Olefins from CO_2 Conversion via Bifunctional Catalysis, ACS Catal. 8 (2018) 571–578, https://doi.org/10.1021/acscatal.7b02649.
[35] Z.R. Catalyst Technical Data Sheet ZR Catalyst. 1–2.
[36] M. Yang, D. Fan, Y. Wei, et al., Recent Progress in Methanol-to-Olefins (MTO) Catalysts, Adv. Mater. 31 (2019) 1–15, https://doi.org/10.1002/adma.201902181.
[37] A.D. Chowdhury, K. Houben, G.T. Whiting, et al., Initial Carbon–Carbon Bond Formation during the Early Stages of the Methanol-to-Olefin Process Proven by Zeolite-Trapped Acetate and Methyl Acetate, Angew. Chem. - Int Ed. 55 (2016) 15840–15845, https://doi.org/10.1002/anie.201608643.
[38] D. Chen, H.P. Rebo, A. Grønvold, et al., Methanol conversion to light olefins over SAPO-34: Kinetic modeling of coke formation, Microporous Mesoporous Mater. 35–36 (2000) 121–135, https://doi.org/10.1016/S1387-1811(99)00213-9.
[39] M. Ronda-Lloret, G. Rothenberg, N.R. Shiju, A Critical Look at Direct Catalytic Hydrogenation of Carbon Dioxide to Olefins, ChemSusChem 12 (2019) 3896–3914, https://doi.org/10.1002/cssc.201900915.
[40] S.S. Arora, A. Bhan, The critical role of methanol pressure in controlling its transfer dehydrogenation and the corresponding effect on propylene-to-ethylene ratio during methanol-to-hydrocarbons catalysis on H-ZSM-5, J. Catal. 356 (2017) 300–306, https://doi.org/10.1016/j.jcat.2017.10.014.
[41] S.S. Arora, Z. Shi, A. Bhan, Mechanistic Basis for Effects of High-Pressure H2 Cofeeds on Methanol-to-Hydrocarbons Catalysis over Zeolites, ACS Catal. 9 (2019) 6407–6414, https://doi.org/10.1021/acscatal.9b00969.
[42] Y.J. Lee, S.C. Baek, K.W. Jun, Methanol conversion on SAPO-34 catalysts prepared by mixed template method, Appl. Catal. A Gen. 329 (2007) 130–136, https://doi.org/10.1016/j.apcata.2007.06.034.
[43] S. Guo, S. Wang, W. Zhang, et al., Catalytic performance of various zinc-based binary metal oxides/H-RUB-13 for hydrogenation of CO_2, Ind. Eng. Chem. Res 61 (2022) 10409–10418, https://doi.org/10.1021/acs.iecr.2c00160.
[44] W. Zhou, K. Cheng, J. Kang, et al., New horizon in C1 chemistry: Breaking the selectivity limitation in transformation of syngas and hydrogenation of CO_2 into hydrocarbon chemicals and fuels, Chem. Soc. Rev. 48 (2019) 3193–3228, https://doi.org/10.1039/c8cs00502h.
[45] S. Gao, S. Xu, Y. Wei, et al., Insight into the deactivation mode of methanol-to-olefins conversion over SAPO-34: Coke, diffusion, and acidic site accessibility, J. Catal. 367 (2018) 306–314, https://doi.org/10.1016/j.jcat.2018.09.010.
[46] Z. Shi, A. Bhan, Methanol-to-olefins catalysis on window-cage type zeolites/zeotypes with syngas co-feeds: Understanding syngas-to-olefins chemistry, J. Catal. 413 (2022) 913–922, https://doi.org/10.1016/j.jcat.2022.07.035.
[47] Z. Chen, Y. Ni, Y. Zhi, et al., Coupling of Methanol and Carbon Monoxide over H-ZSM-5 to Form Aromatics, in: Angew Chemie - Int Ed, 57, 2018, pp. 12549–12553, https://doi.org/10.1002/anie.201807814.